Proceedings of the 21st ICSMGE, Vienna, Austria, 14 – 19 June 2026. Pistrol, Adam & Schweiger (eds.)
Published by: ÖGG, Austrian Society for Geomechanics, Salzburg, Austria, ISBN 978-3-9503898-4-5
https://doi.org/10.53243/ICSMGE2026-1721

Three-dimensional numerical modelling of Swift Anchor for offshore renewable energy applications

Matteo Ciantia, Wei Wang, Marco Previtali
School of science and engineering, University of Dundee, UK, m.o.ciantia@dundee.ac.uk

Nicholas Kaufmann & Nick Cresswell
SCHOTTEL Marine Technologies

ABSTRACT: Rock anchors are essential for the deployment of offshore renewable energy (ORE) systems in rocky seabed conditions. Conventional rock anchors that rely on cement-based grouting can be costly and environmentally challenging, particularly in deep-water applications. Emerging groutless self-drilling anchor technologies, such as the Swift Anchor (SA), present a promising alternative by minimising seabed disturbance and installation risks. Tensile resistance of the SA is from the mechanical interlock between the finger at the end of the anchor and the surrounding rock mass, where a pretension can be applied on the anchor head to enhance the anchor loading response. This paper develops a FLAC3D model to simulate the performance of rock anchors under combined vertical and horizontal (V-H) loading. The rock is modelled using a Hoek-Brown constitutive model, while the anchor is modelled as an elastic material. A simplified method is proposed to explicitly replicate the pretension procedure. The stiffness of load – displacement response is maximised at a loading direction of 45°, decreasing as the direction deviates from this angle. Yield limit and ultimate capacity are relatively insensitive to loading direction, suggesting the potential for a standardised SA design across a range of loading directions under the investigated ground conditions.

KEYWORDS: FLAC3D, rock, anchor, offshore renewable energy

1 INTRODUCTION

Offshore renewable energy (ORE), e.g. offshore wind, has been deemed as a key enabler in achieving the targets of transition to a sustainable energy future. To meet the net-zero aims of the Paris Agreement, 380 GW and 2000 GW of offshore wind are estimated to be required worldwide by 2030 and 2050, respectively. The EU aims to contribute least 340 GW of offshore renewable energy by 2050, which is an increase in capacity by ten compared to the total capacity by 2024 (European Commission 2020; WindEurope 2025).

Some of the planned ORE applications are going to be deployed in rocky seabed locations and therefore the development of efficient and cost-effective anchor solutions is required. To sustain tensile loads, conventional anchor solutions require the use of cement-based grouts (Brown 2015; Finnie et al. 2019; Grindheim et al. 2023). Their use in deeper waters is therefore problematic as installation and decommissioning become extremely difficult and costly. Alternatively, groutless rock anchoring solutions are becoming more attractive for floating ORE applications (ORE Catapult and ARUP 2024).

The rock anchor technology, "Swift Anchor" (SA), investigated in this paper was recently designed by SCHOTTEL Marine Technologies (SMT) (https://schottel-mt.com/) aiming to reduce operation costs and environmental footprint by means of a groutless, and self-drilling solution. This technology relies on the mechanical interlock between rock and anchor to provide stability in weak and hard rocks. The mechanical interlock is similar to that of undercut anchors, which are typically used in steel-concrete connections (Cook et al. 1989) and can be also used in rocks(Jonak et al. 2021).

The main components of the SA include an outer casing with expandable fingers at the base, an upper taper, an anchor nut, and an inner stem fitted with a sacrificial drill bit (Figure 1). The taper has a pad eye which allows the connection between anchor and floating platforms generally through mooring lines. The installation of the anchors is as follow: i) The drill bit cores the rocky seabed to create a cavity for anchor placement, while minimising seabed disturbance and cost of installation. At the drilling stage the inner stem and outer casing are tightened together acting as a single element (Figure 1b). ii) Once reaching the design depth, inner and outer casing are decoupled. The inner stem is retracted expanding the fingers, undercutting the surrounding rock (Figure 1c). This enables full contact between rock and fingers, whereas a gap between shaft and rock remains. iii) Pre-tensioning is then applied by tightening the anchor nut on top ensuring the anchor stability (Figure 1c). This anchoring system also has a potential of reuse by releasing the pre-tension followed by lowering the inner stem and retrieving.

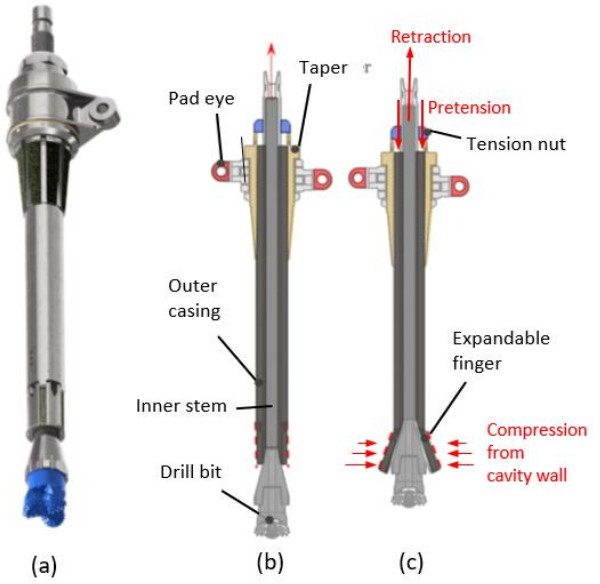

Figure 1. (a) 3D visualisation of the Swift Anchor, and schematic illustration of the installation process: (b) before inner stem retraction and (c) after inner stem retraction

The SA has been recently investigated by means of full-scale field tests (Kaufmann et al. 2025) and reduced-scale laboratory tests (Genco et al. 2024a). Alongside the experimental studies, numerical investigations have been conducted to offer insights into mechanisms controlling the loading behaviours of the SA (Cerfontaine et al. 2021; Genco et al. 2023a, 2023b; Genco et al. 2024b). However, the previous numerical studies focused single loading directions (solely

vertical or lateral), ignoring the multi-directional nature of mooring force (depending on the mooring line setup). In addition, the pad-eye (i.e. loading eccentricity) and the pretension were not simulated for simplification. Validated against field tests, this paper developed a three-dimensional numerical model using Finite Difference software FLAC3D (Itasca 2025) to simulate the pre-tensioning process and investigated multi-directional loading response of the full SA.

2 NUMERICAL MODELLING

2.1 *Rock properties and constitutive parameters*

Mudstone/siltstone at the SA field-testing site at Dörth, Rhineland-Palatinate, Germany was simulated (Kaufmann et al. 2025). The field tests have proofed that the SA provides designed holding resistance. This numerical study, validated against the field tests, is aimed to investigate the SA to failure which could not be achieved in the field due to the high loads required. To model the rock the Hoke-Brown constitutive model was employed by calibrating its parameters against an experimental campaign performed at the geomechanics laboratory of Milano Bicocca. High pressure triaxial tests, unconfined compression tests and Brazilian tests of intact Dörth rock samples were used to identify the failure envelop and the elastic properties of the intact rock. These combined to the site investigation data were used to characterise the rockmass parameters that are summarised in Table 1.

The rock-anchor interface was simulated as a frictional contact by using a non-dilative Mohr-Coulomb constitutive model (see parameters in Table 2). The stiffness parameters i.e. Young's modulus and Poisson's ratio were assumed to be consistent with those for the rock mass Table 1. The interface friction angle was used to be 26°, which is typical for rock-steel interfaces (Ziogos et al. 2017; Ziogos et al. 2023).

Table 1. Hoke-Brown parameters for rock at the testing site, Dörth

Parameter	Symbol	Value	Unit
Young's modulus	E	3.25	GPa
Poisson's ratio	ν	0.3	-
Unconfined	USC	6.3	MPa
Material constant	m_i	9	-
Geological Strength Index	GSI	50	-
Dilation angle	ψ	5.0	°

Table 2. Mohr-Coulomb parameters for Dörth rock – anchor interface

Parameter	Symbol	Value	Unit
Young's modulus	$E_{r\text{-}a}$	3.25	GPa
Poisson's ratio	$N_{r\text{-}a}$	0.3	-
Friction angle	φ	26	°
Dilation angle	$\Psi_{r\text{-}a}$	0	°

2.2 *Anchor model*

Figure 2(a) shows the dimension of the anchor simulated. Pretension is applied by tensioning the inner stem whilst reaction on the top taper. Once pretentions reached the desired value the anchor nut is tightened against the taper. In the field, pretension is maintained through the mechanical interlock between the threads of the nut and the inner stem. In the numerical model, the outer casing and inner stem were modelled as a single component (Figure 2b, dark grey), pretension was maintained by fixing the interface between the top taper and the inner stem avoiding to explicitly modelling the tension nut. The anchor model was linear elastic, with typical steel parameters (Table 3).

To simulate the pretension, a simplified two-phase method was used. First, the top taper an inner stem interface was set to have zero friction (smooth interface), and the inner stem was pulled by the pretension force while the equal and opposite force weas imposed to the top taper. In this phase the fingers of the SA react against the rock until equilibrium is attained.

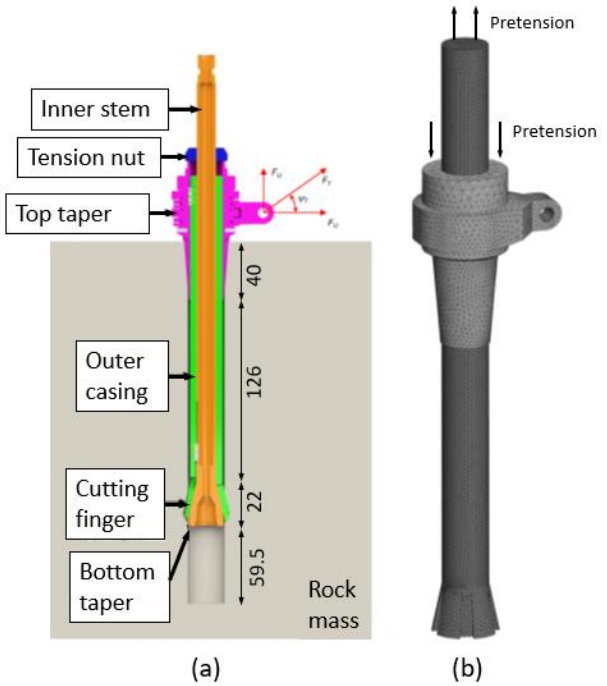

Figure 2. (a) SA dimensions (unit: cm) (b) numerical anchor model mesh and schematic of pretension

In the second phase, the interface strength parameters were increased to arbitrarily high values, creating a perfectly bonded condition to simulate the locking of the tension nut. Then the relaxion is simulated by removing the previously applied forces on the taper and shaft, followed by solving the model to equilibrium again. Section 4.1 will show the pretension phases as described.

Table 3. Anchor and taper-shaft interface parameters

Parameter	Symbol	Value	Unit
Young's modulus	$E_{t\text{-}s}$	200	GPa
Poisson's ratio	$N_{t\text{-}s}$	0.3	-
Friction angle	$\varphi_{t\text{-}s}$	0 or inf	°
Tensile strength	$T_{t\text{-}s}$	0 or inf	GPa
Dilation angle	$\Psi_{t\text{-}s}$	0	°

3 SIMULATION PROGRAM

The simulation program includes different loading conditions to investigate the evolution of pretension and the SA capability to withstand combined loading. Force-controlled monotonic loading tests are conducted until geomechanical failure. The parametric numerical study aims to identify: i) the elastic (yield) envelope, ii) the ultimate yield envelope. Monotonic loading tests were performed at the following angles: Ψ = [90, 45, 0, −90]. Compressive loading scenarios were also simulated, considering the potential application of the SA for fixed-bottom

ORE foundations, such as serving as a single leg of a jacket structure.

4 RESUSLTS

4.1 *Pretension phase*

Figure 3shows the relationship between pretension force and stem vertical displacement, incorporating Dorth field test data (Kaufmann et al. 2025). Figure 4 shows the evolution of pretension throughout the simulation steps. At the beginning of the relaxion phase, the pretension exhibits a sudden drop followed by a partial recovery where the pretension is stabilised at 233 kN.

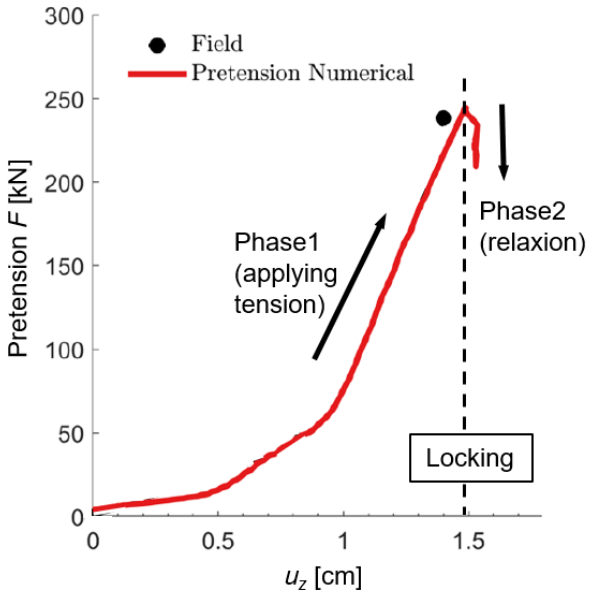

Figure 3. Pretension force vs stem vertical displacement including Dorth filed test data

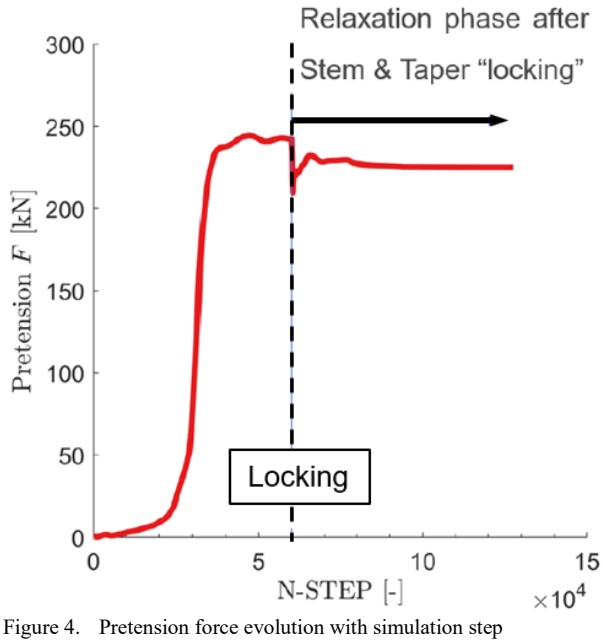

Figure 4. Pretension force evolution with simulation step

Figure 5 shows the significant stress locked below the top taper and above the bottom finger and a stress arch formed between the taper and the finger.

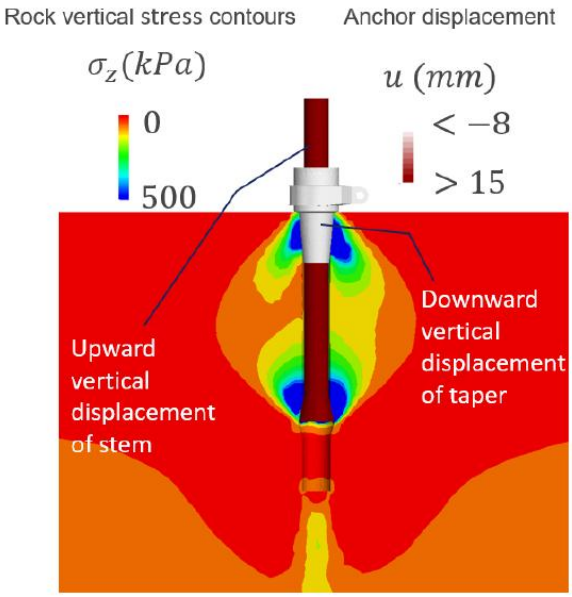

Figure 5. Rock mass vertical stress contours at end of the pretension process

4.2 *Multi-direction monotonic loading results*

Figure 6 shows the shape of failure mechanism for the vertical tensile case ($\Psi = 90°$) by means of plastic strain contours in the rock mass. The mechanism is similar to the cone-shaped failure typically observed for undercut anchors in concrete (Cook et al. 1989), or 'rock mass uplift' failure for grout rock anchors (Brown 2015). By approximating the failure cone boundary as a straight line, an inclination angle of 42° is observed, which is in good agreement with the commonly assumed value of 45° for concrete (Cook et al. 1989). Previous limit analysis of the SAs in rocks suggested that the inclination angles increased with a reduction of Geological Strength Index (GSI) and an increase in anchor embedment depth (Cerfontaine et al. 2021).

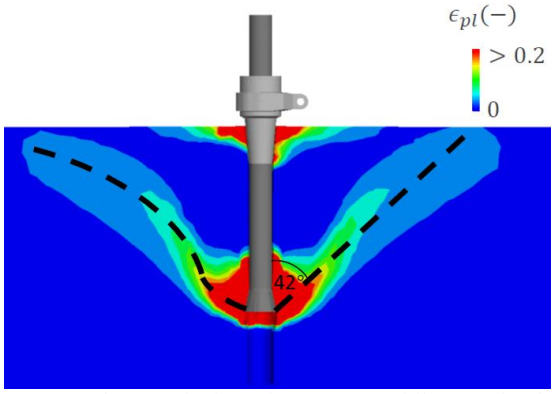

Figure 6. Rock mass plastic strain contours at failure (anchor head uplift $u_V = 8$ cm)

Figure 7 shows the monotonic tensile response at selected loading directions. For each load-displacement curve a yield point (point of inflection of the curve) and the ultimate load (failure, maximum capacity) were identified. These values are then used to construct Yield and Failure envelopes in the Vertical, Horizontal (V-H) force plane (Figure 8).

Across loading directions investigated, the loading direction of 45° produces the stiffest load–displacement response, with stiffness decreasing as the loading direction deviates either above or below this angle. However, only limited differences of yield limits and ultimate capacities are

observed with variation of loading directions. Therefore, the yield and failure envelope determined on the V- H plane only has a minimal eccentricity This may suggest the possibility of a standardised SA design across various loading directions, at least under the rock bed conditions investigated herein.

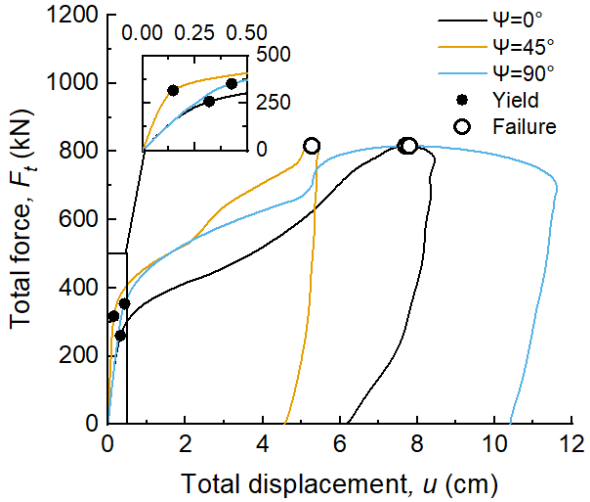

Figure 7. Force – displacement response of the SA during tension tests at $\Psi = 0$, 45 and 90°

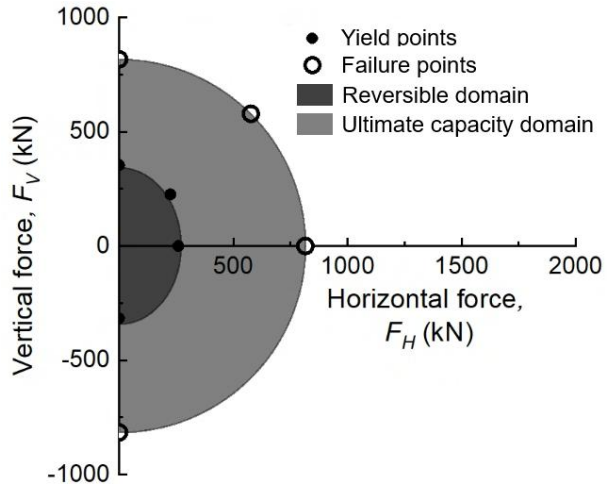

Figure 8. Yield and failure envelopes in the V-H force plane

5 CONCLUSIONS

Using three-dimensional numerical modelling, this paper investigated muti-directional response of a type of novel groutless self-drilling anchor, the Swift Anchor, for ORE applications.

The proposed numerical model adopted a simple approach to replicate the essential pretension process for the Swift Anchor. Loading direction of 45° leads to maximised stiffness of load – displacement response with stiffness decreasing as the loading direction deviates either above or below this angle. However, the variation of yield limit and ultimate capacity with loading direction is limited, leading to a minimal eccentricity of the failure envelope V-H plane. This suggests the potential for a standardised SA design across a range of loading directions under the investigated ground conditions.

6 ACKNOWLEDGEMENTS

This work is an output from the RockMOOR project, funded by the Supergen Offshore Renewable Energy (ORE) Hub through the Flexible Funding scheme (FF2024-1076 – Effect of creep and tensile cyclic loads on serviceability of rock anchoring systems for floating ORE mooring).

7 REFERENCES

Brown, E.T. 2015. Rock engineering design of post-tensioned anchors for dams – A review. Journal of Rock Mechanics and Geotechnical Engineering, **7**(1): 1-13. doi:10.1016/j.jrmge.2014.08.001.

Cerfontaine, B., Brown, M., Caton, A., Hunt, A., and Cresswell, N. 2021. Numerical modelling of rock anchor uplift capacity for offshore applications. *In* 14th European Wave & Tidal Energy Conference, Plymouth, UK.

Cook, R.A., Doerr, G.T., and Klingner, R.E. 1989. Design guide for steel-to-concrete connections.

European Commission. 2020. An EU Strategy to harness the potential of offshore renewable energy for a climate neutral future. Communication from the Commissionto the European Parliament, the Council, the European Economic and Social Committee and the Committee of the Regions: An EU Strategy to harness the potential of offshore renewable energy for a climate neutral future.

Finnie, I., Gillinder, R., Richardson, M., Erbrich, C., Wilson, M., Chow, F., Banimahd, M., and Tyler, S. 2019. Design and Installation of Mobile Offshore Drilling Unit Mooring Piles using Innovative Drive-Drill-Drive Techniques. *In* 13th Australia - New Zealand Conference on Geomechanics, Perth, Australia.

Genco, A., Ciantia, M.O., Previtali, M., Brown, M., Ivanovic, A., and Cresswell, N. 2023a. G-PFEM Numerical Assessment of Rock Anchor Interface Properties on Pull-Out Capacity for Renewable Offshore Applications. *In* 8th Italian Conference of Researchers in Geotechnical Engineering - Geotechnical Engineering in the Digital and Technological Innovation Era. Springer Nature, Palermo, Italy.

Genco, A., Ciantia, M.O., Previtali, M., Brown, M., Ivanovic, A., and Cresswell, N. 2023b. Numerical study of the lateral response of offshore rock anchors. *In* 9th International Offshore Site Investigation and Geotechnics Conference: Innovative Geotechnologies for Energy Transition, London, UK.

Genco, A., Ciantia, M.O., Previtali, M., Brown, M.J., Ivanovic, A., Cresswell, N., and Twomey, V. 2024a. A small-scale physical model for evaluating the axial response of Rock Anchors for offshore renewable applications. *In* 5th European Conference on Physical Modelling in Geotechnics, Delft, the Netherlands.

Genco, A., Ciantia, M.O., Previtali, M., Brown, M., Ivanovic, A., Cresswell, N., and Twomey, V. 2024b. Large deformation numerical assessment of rock anchor response under axial loading for offshore renewable energy applications. Computers and Geotechnics, **173**. doi:10.1016/j.compgeo.2024.106563.

Grindheim, B., Li, C.C., Høien, A.H., and Lia, L. 2023. Behavior of a Rock Mass in Uplift Field Tests of Rock Anchors. Rock Mechanics and Rock Engineering, **57**(4): 2339-2364. doi:10.1007/s00603-023-03689-2.

Itasca Consulting Group, Inc. (2025). FLAC3D – Fast Lagrangian Analysis of Continua in Three-Dimensions, Ver. 9.0

Jonak, J., Karpinski, R., Wojcik, A., and Siegmund, M. 2021. The Influence of the Physical-Mechanical Parameters of Rock on the Extent of the Initial Failure Zone under the Action of an Undercut Anchor. Materials (Basel), **14**(8). doi:10.3390/ma14081841.

Kaufmann, N., Jeffcoate, P., Cresswell, N., and Ciantia, M. 2025. Full-Scale Load Testing of the Swift Rock Anchor. *In* 16th European Wave and Tidal Energy Conference, Madeira, Portugal.

ORE Catapult, and ARUP. 2024. Floating offshore wind anchor review. PN000585-RPT-005 - Rev. 01.

WindEurope. 2025. Wind energy in Europe - 2024 Statistics and the outlook for 2025-2030.

Ziogos, A., Brown, M., Ivanovic, A., and Morgan, N. 2017. Chalk-steel interface testing for marine energy foundations. Proceedings of the Institution of Civil Engineers-Geotechnical Engineering, **170**(3): 285-298. doi:10.1680/jgeen.16.00112.

Ziogos, A., Brown, M.J., Ivanovic, A., and Morgan, N. 2023. Understanding rock-steel interface properties for use in offshore applications. Proceedings of the Institution of Civil Engineers-Geotechnical Engineering, **176**(1): 27-41. doi:10.1680/jgeen.20.00183.